A Molecular Coupling Mechanism for the Oxaloacetate Decarboxylase Na^+ Pump As Inferred from Mutational Analysis†

Petra Jockel, Markus Schmid, Julia Steuber, and Peter Dimroth*

Mikrobiologisches Institut, Eidgenössische Technische Hochschule, ETH-Zentrum, Schmelzbergstrasse 7, CH-8092 Zürich, Switzerland

Received September 28, 1999; Revised Manuscript Received November 18, 1999

ABSTRACT: The oxaloacetate decarboxylase Na^+ pump consists of subunits α, *β*, and *γ*, and contains biotin as the prosthetic group. Membrane-bound subunit *β* catalyzes the decarboxylation of carboxybiotin coupled to Na^+ translocation, and consumes a periplasmically derived proton. Site-directed mutagenesis of conserved amino acids of transmembrane helix VIII indicated that residues N373, G377, S382, and R389 are functionally important. The polar side groups of these amino acids may constitute together with D203 a network of ionizable groups which promotes the translocation of Na^+ and the oppositely oriented H^+ across the membrane. Evidence is presented that two Na^+ ions are bound simultaneously to subunit *β* during transport with D203 and S382 acting as binding sites. Sodium ion binding from the cytoplasm to both sites elicits decarboxylation of carboxybiotin, and a conformational switch exposes the bound Na^+ ions toward the periplasm. After dissociation of Na^+ and binding of H^+, the cytoplasmically exposed conformation is regained.

Oxaloacetate decarboxylase of *Klebsiella pneumoniae* is the prototype for the sodium ion transport decarboxylase family of enzymes, which also includes methylmalonyl-CoA decarboxylases, malonate decarboxylase, and glutaconyl-CoA decarboxylases from various anaerobic bacteria. These enzymes use the free energy of the decarboxylation reactions to pump Na^+ ions across the membrane (*1*−*3*). The resulting $\Delta\tilde{\mu}Na^+$ drives active transport reactions or the synthesis of ATP. The latter process has been termed decarboxylation phosphorylation and is the only ATP-generating mechanism in *Propionigenium modestum* or *Malonomonas rubra*, which grow from the decarboxylation of succinate to propionate or malonate to acetate, respectively (*4*, *5*).

The oxaloacetate decarboxylase Na^+ pump of *K. pneumoniae*, whose overall geometry and function is shown in Figure 1A, is composed of three different subunits, α, *β*, and *γ* (OadA, -B, and -G), with molecular masses of 63.5, 44.9, and 8.9 kDa, respectively (*1*, *2*, *6*−*8*). The peripheral α-subunit consists of two domains, the N-terminal carboxyltransferase domain and the C-terminal biotin-binding domain, which are connected by a flexible proline/alanine linker (*8*). The *β*-subunit comprises the main membrane integral portion of the enzyme complex. It folds into an N-terminal block of three membrane-spanning α-helices and a C-terminal block of six membrane-spanning α-helices. The connecting fragment consists of two loops that insert from the periplasm into the membrane, but do not reach the cytoplasmic surface (*9*; Figure 1B). The second of these membrane-integral loops carries the invariant D203 residue, which is crucial for catalytic activity and resides within the most highly conserved area of OadB (*10*). The *γ*-subunit is anchored in the membrane with a single N-terminal α-helix. This is succeeded on the cytoplasmic surface by a proline/alanine linker and a short hydrophilic domain harboring three conservative

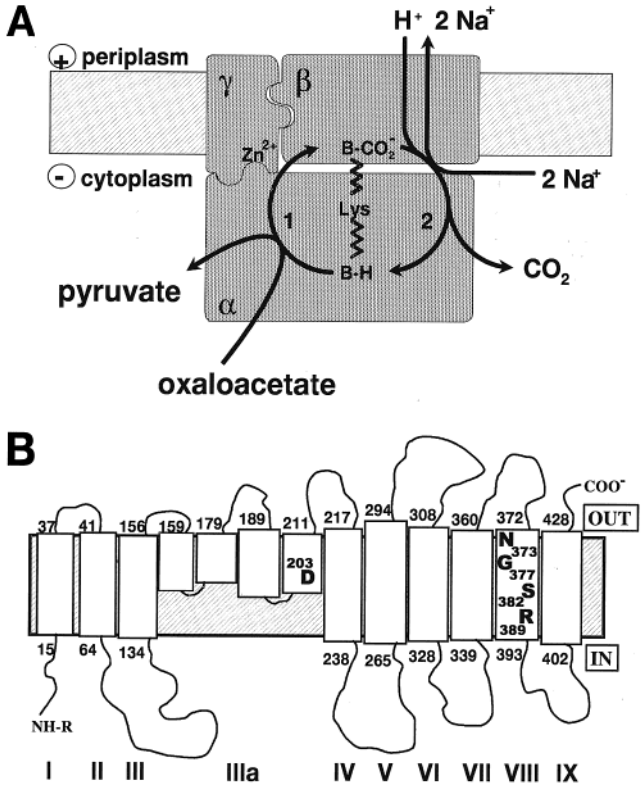

FIGURE 1: (A) Cartoon showing the overall geometry of the oxaloacetate decarboxylase and features of the catalytic events. B-H is biotin, $B\text{-}CO_2^-$ carboxybiotin, Lys the biotin-binding lysine residue, 1 the carboxyltransferase reaction, and 2 the decarboxylase reaction; for details, see the text. (B) Topology model for OadB emphasizing functionally important amino acid residues.

† This work was supported by the Swiss National Science Foundation.

* Corresponding author. E-mail: dimroth@micro.biol.ethz.ch. Telephone: 0041 1 632 33 21. Fax: 0041 1 632 13 78.

10.1021/bi992261v CCC: $19.00 © 2000 American Chemical Society
Published on Web 02/12/2000

histidines near the C-terminus. These histidines are likely ligands for the Zn^{2+} ion associated with it. The β- and γ-subunits form a subcomplex which associates with the α-subunit (*11*−*14*).

The catalytic reaction cycle starts with the carboxyl transfer from oxaloacetate to the prosthetic biotin group. This reaction step is catalyzed at a low rate (0.13 s^{-1}) by the α-subunit alone. This rate is enhanced approximately 1000-fold within the oxaloacetate decarboxylase complex, probably because the Zn^{2+} metal ion of the γ-subunit polarizes the carbonyl oxygen bond of oxaloacetate, thereby promoting the carboxyl transfer to biotin (*11*, *14*). Facilitated by the flexible proline/alanine linker, the carboxybiotin switches from the carboxyl transfer site at the α-subunit to the decarboxylase site at the β-subunit (*8*). In the course of the subsequent decarboxylation reaction, two Na^+ ions are pumped into the periplasm, and one H^+ traverses the membrane in the opposite direction. This proton is consumed during the release of CO_2 from the biotin carboxylate. Switching the biotin back to the carboxyltransferase site completes the cycle (*10*).

Previous site-directed mutagenesis studies indicated that the universally conserved D203 residue of OadB is absolutely essential for the Na^+ transport and decarboxylase activities, but not for the carboxyltransferase activity. On the basis of these and other results, a direct coupling mechanism was proposed, in which D203 plays an essential role in both the vectorial and the chemical reaction. In the proposed mechanism, the protonated D203 residue takes up a Na^+ ion with the proton moving simultaneously to the carboxybiotin and catalyzing the immediate decarboxylation of this acid-labile compound (*10*).

Next to the region around βD203, the most highly conserved area is within a hydrophobic stretch near the C-terminus, which was shown by topology analysis to form transmembrane (TM) helix VIII (*9*; Figure 1B). We have used an *Escherichia coli* expression clone harboring the three genes for the oxaloacetate decarboxylase on plasmid pSK-GAB (*11*) to replace highly conserved amino acids within TM-helix VIII of OadB. The phenotypic characterization of the derived mutants confirmed that this region of OadB is essential for catalytic activity, identifying N373, G377, S382, and R389 as amino acids with primary importance for function.

EXPERIMENTAL PROCEDURES

Bacterial Strains and Plasmids. The bacterial strains used in this study are *E. coli* DH5α (Bethesda Research Laboratories), *E. coli* JM110 (*15*), *E. coli* EP432 (*16*), and *E. coli* BL21(DE3)pLysS (*17*). All strains, except *E. coli* EP432, were routinely grown at 37 °C in Luria Bertani (LB) medium (*18*). *E. coli* EP432 was grown in 20 mM glucose, 50 mM potassium phosphate (pH 5.9), 18.7 mM ammonium chloride, 43 mM potassium sulfate, 1 mM magnesium sulfate, 0.1 mM calcium chloride, 0.1 mg/mL threonine, 2.5 μg/mL thiamin, and either 50, 260, or 360 mM sodium chloride at 30 °C. Plasmid-containing strains were supplemented with the selective antibiotics ampicillin (100 μg/mL) and/or chloramphenicol (40 μg/mL) or kanamycinsulfate (50 μg/mL). Plasmid pSK-GAB was prepared as described previously (*11*). Plasmid pSK^+ was purchased from MBI Fermentas.

Recombinant DNA Techniques. Standard recombinant DNA techniques were performed essentially as described previously (*18*). Polymerase chain reactions (PCRs) were performed using Vent-DNA-Polymerase from New England Biolabs (Beverly, MA). DNA sequencing was carried out according to the dideoxynucleotide chain-termination method (*19*) using a *Taq* DyeDeoxy terminator cycle kit and the ABI Prism 310 genetic analyzer from Applied Biosystems.

Construction of Site-Directed Mutants of the β-Subunit. The primers used for site-directed mutagenesis are listed in Table A of the Supporting Information. Site-directed mutants were obtained as follows. The PCR fragments containing the mutations were constructed in a two-step protocol. For the N-terminal part of the PCR fragments of the β-subunit, primer prBN and primers with the affix rev were used, and pSK-GAB (*11*) served as the template. For the corresponding C-terminal part of the PCR, primer prBC and primers with the affix for were used, and pSK-GAB (*11*) served as the template. After purification, those PCR fragments were used as the template for the PCR products from primer prBN and prBC, which contained the mutation. PCR products were digested with *Bcl*I and *Bst*1107I and cloned into pSK-GAB. From pSK-GAB, which was isolated from JM110 cells, the *Bcl*I−*Bst*1107I fragment was removed.

Purification of Oxaloacetate Decarboxylase Mutants and Enzyme Assays. Oxaloacetate decarboxylase mutants were purified from DH5α/pSK-GAB variants by affinity chromatography of a solubilized membrane extract on a SoftLink monomeric avidin−Sepharose column (Promega) (*20*). Large-scale purification was performed according to ref *10*. The decarboxylation activity was determined with the simple spectrophotometric assay at 265 nm as described previously (*20*).

Screening of Oxaloacetate Decarboxylase Activity of Mutant Clones. Before a large-scale purification of a mutant protein was performed, a small-scale culture of the respective clone was used to measure oxaloacetate decarboxylase activity (*10*). Another method that was used was transformation of the mutant plasmid into *E. coli* EP432, which lacks both Na^+/H^+ antiporters and is therefore unable to grow in the presence of 360 mM NaCl (*16*). In the presence of an active oxaloacetate decarboxylase Na^+ pump, however, the strain resumes growing under these conditions (see Figure 4). This is therefore a convenient assay for the in vivo function of the Na^+ pump.

Labeling of Oxaloacetate Decarboxylase and Mutant Enzymes with $^{14}CO_2$ from [4-^{14}C]Oxaloacetate. [4-^{14}C]-Oxaloacetate, prepared from [4-^{14}C]-L-aspartate and α-oxoglutarate with glutamate:oxaloacetate transaminase, was used to assess the transfer of the radioactive carboxyl residue to biotin bound to OadA as described previously (*11*). The radiolabeled protein was separated from excess substrates after incubation for 10 min in a Sephadex G-25 column in 100 mM Tris/HCl buffer (pH 8.5). Fractions of 400 μL were collected, and the amount of radioactivity was determined by liquid scintillation counting.

Determination of Oxaloacetate Decarboxylase Activity at Various Na^+ Concentrations and pH Values. The decarboxylation activity of wild-type (DH5α/pSK-GAB) and mutant oxaloacetate decarboxylases was measured at different pH values in the range between pH 5.5 and 8.8 in 40 mM Mes/Tris buffer containing variable Na^+ concentrations with the simple spectrophotometric assay according to ref *20*.

Analytical Procedures. The protein content of samples was determined according to the method of Bradford (*21*) or by the bicinchoninic acid method (*22*).

Effect of Na^+ on Tryptic Hydrolysis of the Oxaloacetate Decarboxylase β-Subunit. The incubation mixtures contained in 60 or 84 μL at 25 °C (mixture A) 20 mM potassium phosphate buffer (pH 7.5), 50 mM potassium chloride, purified wild-type or mutant oxaloacetate decarboxylase (25 or 35 μg), and 3 μg of trypsin. A parallel incubation mixture (B) contained 50 mM sodium chloride instead of potassium chloride. Samples (12 μL) were transferred after incubation for 0 (before addition of trypsin), 2, 4, 7.5, and 24 h or 0 (before adding of trypsin), 15, 30, 45, 60, 90, and 120 min into 1 μL of 50 mM phenylmethanesulfonyl fluoride to inactivate the trypsin and 12 μL of SDS sample buffer. After the samples had been heated to 95 °C for 5 min, they were subjected to 10% SDS−PAGE. The gels were immediately stained with silver. Quantification of the β-subunit bands was performed with the program ImageMaster 1D Prime purchased from Pharmacia/Amersham. Half-times of the β-subunit in the presence of trypsin with or without Na^+ were obtained with the program Sigmaplot.

Analysis of Na^+ Uptake into Membrane Vesicles. Na^+ uptake was followed by atomic absorption spectroscopy as described by Krebs et al. (*23*). Incubation mixtures contained (in 150 μL) membrane vesicles (1.3−1.4 mg of protein) prepared as described in ref *20*, 50 mM potassium phosphate buffer (pH 7.5), 20 mM NaCl, and 7 μM valinomycin. The reaction was started by adding 1 mM oxaloacetate (final concentration). At different times (10 and 30 s), samples of 70 μL were applied to a 1 mL plastic syringe containing 0.6 mL of Dowex 50 (K^+), equilibrated with assay buffer without NaCl. The eluate was collected in plastic tubes, and the amount of Na^+ trapped in the vesicles was determined. Controls were performed without oxaloacetate. The results that are reported are averages from three independent experiments.

RESULTS

Selection of Amino Acids for Site-Directed Mutagenesis. Sequence alignments of OadB with related proteins reveal two highly conserved areas. One of these is the region surrounding D203, and the other is transmembrane helix VIII (*9*; Figure 1B). An alignment of the latter segment, shown in Figure 2A, indicates the presence of nine invariant amino acid residues. We selected polar amino acids N373, S382, R389, and N392 of this domain for mutational analyses, because these residues could participate in the translocation of Na^+ or H^+ across the membrane. In addition, the role of the uniquely conserved glycines at positions 377 and 380 was investigated. In this study, the highly conserved proline residues at positions 374 and 385 were not mutagenized, because prolines are considered to be important structural determinants within hydrophobic segments (*24*).

Synthesis of Mutant Oxaloacetate Decarboxylases in E. coli and Specific Oxaloacetate Decarboxylase Activities. To synthesize the mutant oxaloacetate decarboxylases, mutated DNA fragments were cloned into pSK-GAB (*11*) using appropriate restriction sites and used to transform *E. coli* DH5α, as described in Experimental Procedures. Grown cells were disrupted, and mutant oxaloacetate decarboxylases were

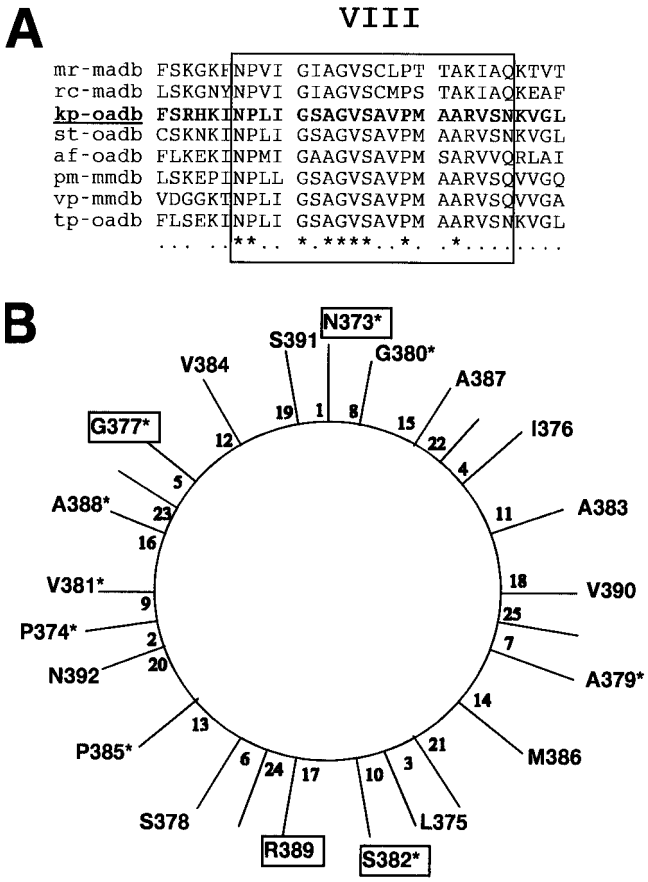

FIGURE 2: (A) Sequence alignment of transmembrane helix VIII (boxed) of the β-subunits of oxaloacetate decarboxylases from *K. pneumoniae* (Kp-OadB), *Salmonella typhimurium* (St-OadB), *Archeoglobus fulgidus* (Af-OadB), and *Treponema pallidum* (Tp-OadB), the related membrane-bound subunits of the Na^+ pumping methylmalonyl-CoA-decarboxylases from *P. modestum* (Pm-MmdB) and *Veillonella parvula* (Vp-MmdB), and the malonate decarboxylases from *M. rubra* (Mr-MadB) and *Rhodobacter capsulatus* (Rc-MadB). Identical residues are denoted with asterisks and conservative exchanges by dots. The sequence of Kp-OadB is given in bold. (B) Helical wheel model of helix VIII. Conserved residues are denoted with asterisks. Functionally important residues are boxed. Small numbers mark the position in the helix.

affinity purified from the solubilized membrane fractions (*20*). The synthesis of the three polypeptide chains of the decarboxylase complexes was verified for all mutants described here by sodium dodecyl sulfate−polyacrylamide gel electrophoresis (SDS−PAGE), and a selection of these analyses is shown in Figure 3. The expression of mutant enzyme complexes was quantified by protein determination, and the data of Table 1 show that between 0.03 and 1 mg of the mutant enzymes could be isolated from 2−3 g of wet packed cells. Also shown in Table 1 are the specific oxaloacetate decarboxylase activities of the isolated mutant enzymes.

By mutation of G377 to A or S382 to A, C, E, N, or Q, the decarboxylase activity was completely abolished, indicating that G377 and S382 are functionally significant. The drastic effect of the G377A mutation on activity is unique to this residue, because several other glycine to alanine mutants, including G380A, retained significant oxaloacetate decarboxylase activities (Table 1, data not shown in part). The S382T mutant retained about 10% of the oxaloacetate decarboxylase activity, and a similar activity was found for

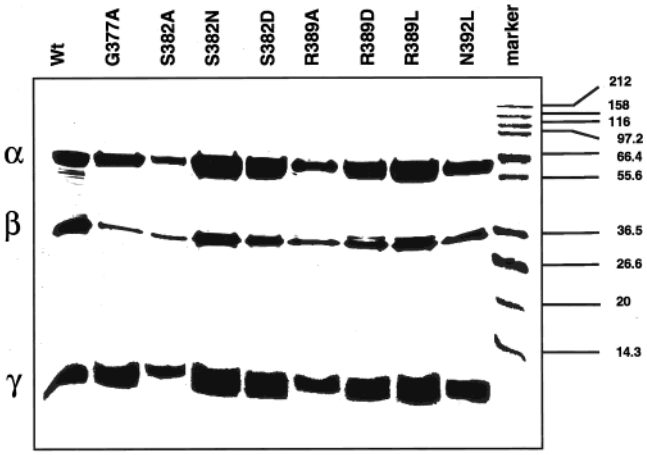

FIGURE 3: Expression of mutant oxaloacetate decarboxylases as evidenced from silver-stained SDS−PAGE after purification of the enzymes. Mutations in OadB are indicated. Wt is the lane with the wild-type enzyme; marker is the lane with marker proteins with molecular masses shown (in kilodaltons). α, *β*, and *γ* denote the three subunits of oxaloacetate decarboxylase.

Table 1: Synthesis of Mutant Oxaloacetate Decarboxylases from OadB Variants and Specific Activities of Isolated Enzymes

mutation	amount of oxaloacetate decarboxylase isolated (mg)[a]	specific activity of isolated oxaloacetate decarboxylase at pH 7.5 (units/mg)
wild-type	1.0	45.4
D203N	1.1	0
N373L	0.03	0.3
G377A	0.3	0
G380A	0.4	14.6
S382A	0.1	0
S382C	0.6	0
S382D	1.0	4.2
S382E	1.1	0
S382N	1.1	0
S382Q	0.6	0
S382T	0.9	3.4
R389A	0.5	3.4
R389D	0.5	0.3
R389K	1.3	35.8
R389L	0.9	4.4
N392L	0.3	31.7

[a] From 2 L of LB culture (2−3 g of wet packed cells).

the S382D mutant. Hence, a protonatable group on a side chain with proper length might be required at position 382 and might cycle between the protonated and unprotonated state (see Discussion). Replacement of R389 with the neutral amino acid A or L reduced the oxaloacetate decarboxylase activity to about 10%. With the conservative R389K exchange, the activity was not significantly affected, but in the mutant with a R389D substitution, the activity dropped below 1%. Other polar residues of helix VIII are N373 and N392, located near the periplasmic and cytoplasmic border, respectively. The N373L mutant enzyme had less than 1% of the activity of the wild-type enzyme, indicating an important functional role for the asparagine residue at position 373. In contrast, the decarboxylase with the N392L substitution only exhibited 30% reduction of activity, and therefore, this asparagine residue is not considered functionally significant.

Formation of Stable Carboxybiotin Enzyme Derivatives with Mutants in OadB Which Are Inactive in Oxaloacetate Decarboxylation. We assumed that enzymes that had been mutated in OadB and yielded an oxaloacetate decarboxylase negative phenotype were not affected in the first partial reaction, i.e., the carboxyl transfer from oxaloacetate to the prosthetic biotin group, because this reaction is catalyzed by OadA. The enzymes with the G377A, S382A, S382C, S382E, S382N, or S382Q mutation became rapidly labeled upon incubation with [4-^{14}C]oxaloacetate, which indicates transfer of the labeled carboxylate to the biotin. The amount of radioactive label acquired by the proteins was approximately 100% of the expected value for all these OadB mutants except for the S382C mutant, where the level of labeling reached 60% (data not shown). As the subsequent decarboxylation of the carboxybiotin enzyme was impaired, Na^+ ions were without effect on the labeling of the enzyme. In contrast, the carboxybiotin-containing protein of the wild-type was only obtained if the presence of Na^+ was carefully excluded (*25*). We conclude, therefore, that in the OadB mutations listed above the carboxybiotin decarboxylase activity was specifically impaired, whereas the carboxyltransferase activity was retained (Figure 1A).

Table 2: Effect of OadB Mutations on Na^+ Binding Characteristics and pH Profiles

mutation	half-maximal activation by Na^+ (mM)	pH optimum	half-time for OadB digestion[a] (with Na^+/without Na^+) (h)
wild-type	0.5	7.0	>24/12
D203N			10/10
N373L	0.7	8.7	nd
G377A			<1/<1
G380A	0.1	6.5−7.0	nd
S382A			nd
S382C			<1/nd
S382D	0.8	6.4	>24/12
S382E			<1/nd
S382N			<1/nd
S382Q			<1/nd
S382T	0.7	8.0	nd
R389A	1.0	8.5	>24 h/12
R389D	nd	6.5	nd
R389K	1.3	6.5	nd
R389L	2.6	9.2	nd
N392L	0.6	6.5	nd

[a] Half-time for digestion of OadB by trypsin in the presence of 50 mM NaCl (with Na^+) or in the absence of Na^+ (without Na^+). nd means not determined.

Tryptic Hydrolysis of Mutant Oxaloacetate Decarboxylases. It has been noted previously that at Na^+ concentrations of 20−50 mM, OadB was specifically protected from tryptic hydrolysis (*13*, *26*). Two different Na^+ binding sites were envisaged, one with high affinity reflected by a half-maximal activation at 0.5 mM and one with an approximately 2 order of magnitude lower binding affinity (*3*, *10*). Occupation of these sites with Na^+ apparently results in a conformational change of OadB, which makes the protein more resistant to tryptic hydrolysis. Under our conditions, the half-time for tryptic digestion of wild-type OadB was 12 h in the absence of Na^+ and >24 h in the presence of 50 mM NaCl. The half-time in the presence of Na^+ dropped to about 1 h for mutants G377A, S382C, S382E, S382N, and S382Q (see Table 2), indicating that these mutant OadBs adopt conformations that are more susceptible to proteolysis. In contrast, OadBs with an S382D or R389A mutation exhibited the wild-type properties with respect to tryptic hydrolysis. Hence, in the structure of these variants, trypsin cleavage sites are

only poorly accessible, so cleavage by trypsin is slow. Furthermore, the Na^+ binding sites are retained, and if these are occupied, OadB is further protected from tryptic digestion. Of particular interest is the catalytically inactive mutant D203N. In this enzyme, the half-time for tryptic digestion was 10 h, close to that of the wild type, but the protective effect of Na^+ ions was missing. On the basis of these data, we propose two Na^+ binding sites in OadB, located at D203 and S382, respectively. Only if both of these sites are present and occupied by Na^+ does OadB change into the conformation where it is highly resistant to proteolysis.

Effect of OadB Mutations on Na^+ Binding Characteristics and pH Profiles. The oxaloacetate decarboxylase is specifically activated by Na^+, with a half-maximal activity at about 0.5 mM. For several OadB mutants, Na^+ activation profiles were determined to check for variations in the Na^+ binding affinity. The results, shown in Table 2, indicate that in the N373L, S382D, S382T, and N392L mutants the half-maximal activation is achieved at slightly higher Na^+ concentrations than in the wild-type enzyme. The affinity for Na^+ decreased 2-, 2.5-, and 5-fold in the R389A, R389K, and R389L mutants, respectively. In the mutant enzyme with the G380A substitution, the half-maximal activation was observed at Na^+ concentrations that were about 5 times lower than in the wild-type decarboxylase and Na^+ inhibition was observed at lower concentrations (>2 mM) than usual (>20 mM) (*10*). For most mutant decarboxylases, the pH optimum was between 6.5 and 7.0, which is similar to that of the wild-type enzyme. Significantly higher pH optima of ≥8.5 were found for the N373L and R389A or R389L mutants. The significance of these results with respect to the ion translocation mechanism will be described in the Discussion.

The mutants were further characterized by their Na^+ pumping activity. For this purpose, we took advantage of the fact that growth of *E. coli* EP432 is impaired by elevated NaCl concentrations due to deletions of both Na^+/H^+ antiporters (*16*). We reasoned that the Na^+ toxicity could be overcome by transforming the cells with plasmid pSK-GAB (*11*), which expresses the Na^+ pumping oxaloacetate decarboxylase. The results of Figure 4 show that this is indeed the case. *E. coli* EP432, transformed with plasmid pSK-GAB, resumed growing on glucose minimal medium, containing 260 or 360 mM NaCl, after a lag phase of approximately 20 h. In contrast, *E. coli* EP432 transformed with the vector (pSK^+) alone or with mutant plasmids, expressing catalytically inactive oxaloacetate decarboxylases, was unable to grow at the elevated NaCl concentrations (Figure 4 and Table 3). It has been noticed that on prolonged incubation of *E. coli* EP432 on LB medium containing elevated NaCl concentrations, spontaneous mutants that start growing under these conditions arise (*27*). In our experiments, however, growth was clearly dependent on the expression of the oxaloacetate decarboxylase Na^+ pump from plasmid pSK-GAB (see above). The results of Tables 1 and 3 indicate that *E. coli* EP432 expressing a mutated oxaloacetate decarboxylase with a specific activity of >3 units/mg of protein (after purification) is generally able to grow in the presence of 360 mM NaCl. Exceptions are the R389A and R389L mutants, which are unable to grow, although their isolated oxaloacetate decarboxylases have specific activities of about 4 units/mg of protein at pH 7.5. Please note that in these mutants, the pH optimum is shifted into the alkaline area (Table 2) and that the growth experiments were performed at pH 5.9, where the specific activities for the R389A and R389L mutants are reduced to 1.8 and 2.6 units/mg of protein, respectively. Less growth is observed for the R389K mutant, despite the good expression and near wild-type specific oxaloacetate decarboxylase activity of the isolated enzyme. Less growth is also observed for the N392L mutant, from which the enzyme with high specific activity was isolated. In this case, however, the reduction in the level of growth might be due to the diminished expression level of the enzyme (Tables 1 and 3).

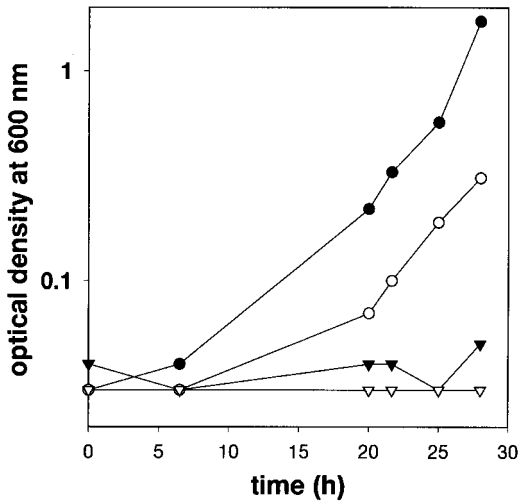

FIGURE 4: Complementation of the Na^+/H^+ antiporter-deficient *E. coli* mutant EP432 with the oxaloacetate decarboxylase from *K. pneumoniae*. Growth was followed at 260 mM NaCl (black symbols) or 360 mM NaCl (white symbols) with *E. coli* EP432 transformed with plasmid pSK-GAB encoding the oxaloacetate decarboxylase (circles) or plasmid pSK^+ as a control (triangles).

Table 3: Growth of *E. coli* EP432 Transformed with Plasmids Expressing Mutant Oxaloacetate Decarboxylases in the Presence of 360 mM NaCl[a]

mutation	optical density at 600 nm[b]
wild-type	0.45
G380A	0.15
S382D	0.22
S382T	0.16
R389K	0.15
N392L	0.10

[a] No growth was observed for mutants N373L, G377A, S382A, S382C, S382E, S382N, S382Q, R389A, R389D, and R389L. [b] The optical density was determined after growth for 28 h at 30 °C.

Dependence of Oxaloacetate Decarboxylase Activity on Na^+ Concentration. The results of site-directed mutagenesis of OadB described above suggested that S382 could act as a binding site for Na^+ during the translocation of the alkali ion across the membrane. From previous studies, D203 and the carboxybiotin were inferred to be putative Na^+ binding sites of OadB (*10*). Two of these sites could be occupied simultaneously, because two Na^+ ions are translocated per decarboxylation event (*14*). We have therefore reinvestigated the dependence of oxaloacetate decarboxylase activity on Na^+ concentration, with special attention paid to cooperativity. The results depicted in Figure 5 clearly show a sigmoid shape of the Na^+ activation profile for oxaloacetate decarboxylase. The experimental data follow the line calculated

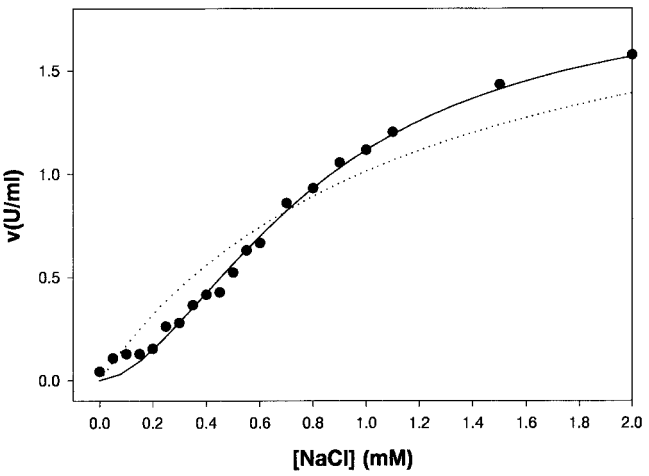

FIGURE 5: Activation profile of wild-type oxaloacetate decarboxylase for activation by Na^+ ions at pH 5.5. Experimental data (●) were fitted according to the Hill (−) or Michaelis−Menten equation (···).

by the Hill equation with an n_H of 1.8, but not that calculated with the Michaelis−Menten equation with a single Na^+ binding site. Neither could our data be fitted to the Michaelis−Menten equation assuming two Na^+ binding sites (not shown). The results indicate that two Na^+ ions have to bind simultaneously to achieve the maximum activity of the enzyme and that the binding of the Na^+ ions is cooperative. The simultaneous binding of two Na^+ ions to OadB is in accord with the observation that the two putative Na^+ binding residues, D203 and S382, must be present to achieve Na^+-dependent protection of the protein from tryptic hydrolysis. We therefore propose that D203 and S382 act as two different Na^+ binding sites in OadB.

DISCUSSION

Recent topological analyses of OadB have indicated that the highly conserved area comprising residues 372−393 folds into transmembrane helix VIII (*9*; Figures 1B and 2). Our mutational studies presented here show that this region harbors several amino acids that are functionally significant. Inactive or nearly inactive enzyme specimens were obtained by mutating βN373 to L, βG377 to A, or βS382 to A, C, E, N, or Q. These OadB mutations specifically affect the carboxybiotin decarboxylase activity of the enzyme, not the carboxyltransferase activity which is intrinsic to OadA (*11*, *26*; Figure 1A). We assume that the carboxybiotin binds near the cytoplasmic surface in the vicinity of helix VIII. The proton, which is consumed during the decarboxylation reaction, stems from the periplasmic reservoir, and two Na^+ ions are pumped into this reservoir from the cytoplasmic compartment (Figure 1A; *10*). Hence, protons and Na^+ ions traverse the membrane in opposite directions, for which they might use the same network of ionizable amino acid residues. Previously, an important role in both Na^+ and H^+ transport has been assigned to D203, which according to the OadB topology is located in the vicinity of the periplasmic surface (*9*, *10*).

We propose a similar role for S382, which is located within helix VIII, close to the center of the membrane. This assumption is based on the fact that for retention of decarboxylase activity, S, T, and D are the only amino acids tolerated at position 382. It is intriguing that the enzyme with the S382D substitution retained approximately 10% of the wild-type activity, whereas that with the S382N mutation was completely inactive. As D and N might be considered about equally suitable as Na^+ binding ligands, we attribute the preference of D over N at position 382 to the protonation and deprotonation of this site during the catalytic cycle. However, if the only role of S382 would be that of a proton carrier, it is difficult to explain why the S382C or S382E mutants are completely inactive. For these reasons, we propose a dual function for S382, serving as a Na^+ binding site during the transport of this alkali ion into the periplasm and as a H^+ binding site for guiding protons in the opposite direction through the membrane into the catalytic site. Hence, S382 could perform a role similar to that of D203 (*10*), and both residues could be part of a Na^+ and H^+ translocation network within the membrane. The proposed role of D203 as a Na^+ binding site residue is in accord with the loss of the Na^+-specific protection of OadB from tryptic hydrolysis in the D203N mutant (see Results).

To function in proton conduction, the side chain hydroxyl of S382 has to switch between the protonated and deprotonated states. In aqueous environments, the hydroxyl group of serine has a p*K* of >13 and therefore does not deprotonate under physiological conditions. However, as exemplified for the serine proteases, abstraction of the proton from serine is feasible with histidine acting as a base within a hydrophobic pocket of the enzyme (for review, see ref *28*). A candidate to take over a proton from S382 in OadB is the R389−carboxybiotin pair. The R389 residue is located two helical turns apart from S382 toward the cytoplasm, and both residues have their side chain exposed to the same side (Figure 2B). Furthermore, R389 is conserved among species, except for the conservative R389K exchanges in the malonate decarboxylase β-subunits (Figure 2A). Mutational analyses reported here support the proposal of an intimate interaction between S382 and R389 in the proton-conducting pathway. While the R389K mutant exhibited almost wild-type oxaloacetate decarboxylase activity and was a functional Na^+ pump, all the other mutants that were investigated had severely reduced decarboxylase and impaired Na^+ pumping activities as judged from growth assays with the Na^+-sensitive *E. coli* EP432 strain. An increase in the pH optimum of the decarboxylase by about 2 units in the R389A or R389L mutant compared to that of the wild type (Table 2) is further in accord with the proposed proton conduction from S382 via R389 to carboxybiotin, where it initiates the decarboxylation of this acid-labile compound.

In the following, we propose a model for the coupling mechanism of the oxaloacetate decarboxylase Na^+ pump that takes present and previous results into account. The model, shown in Figure 6, is significantly distinct from a previous one, in which the simultaneous binding of two Na^+ ions to OadB was not yet recognized (*10*). This was deduced from the Hill coefficient of 1.8 that derived from the Na^+ activation profile of the decarboxylase (see Results). Mutational analyses have identified transmembrane helix VIII and that part of region IIIa surrounding D203 as essential for the decarboxylation of carboxybiotin and for the translocation of Na^+ and H^+ across the membrane that is coupled to it. It is proposed that unliganded OadB switches between conformation 1, in which the Na^+ binding sites are open to the

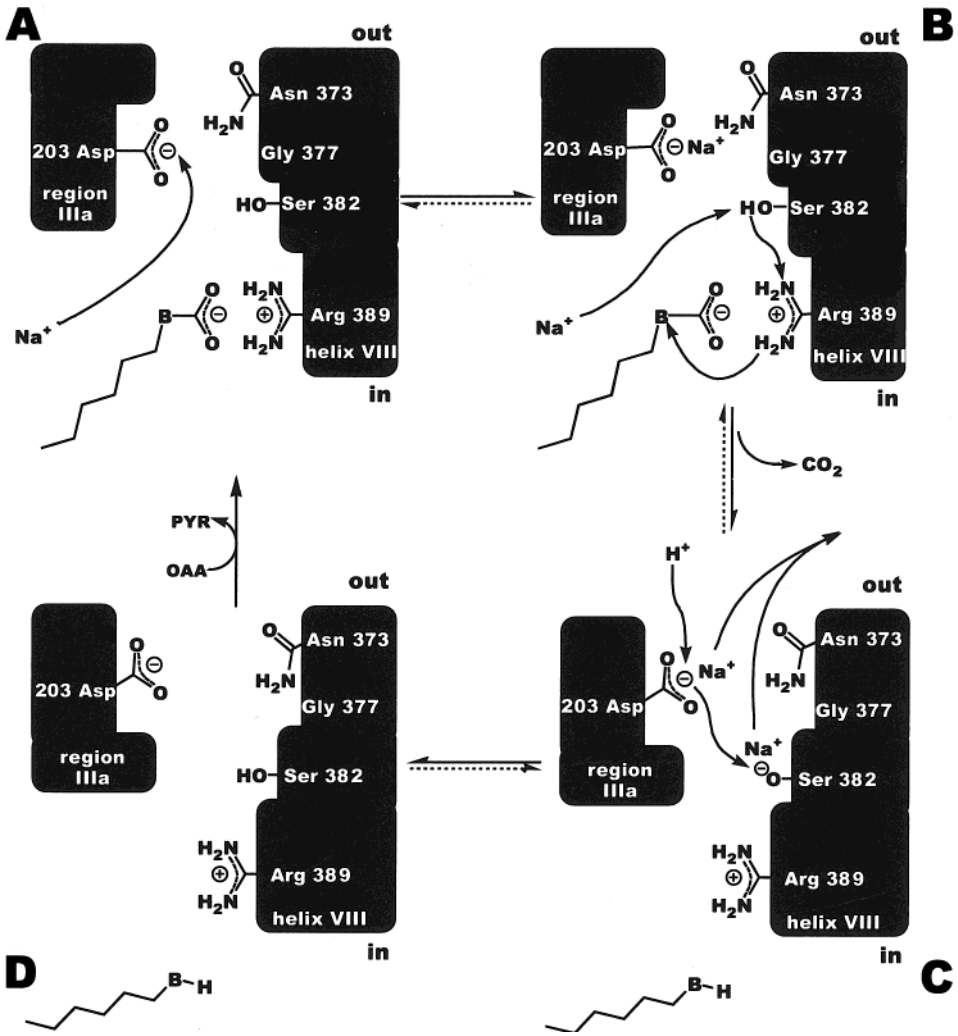

FIGURE 6: Model for coupling Na^+ and H^+ movements across the membrane to the decarboxylation of carboxybiotin. The model shows the approximate location of important residues of helix VIII and region IIIa of the β-subunit. Also shown is the participation of these residues in the vectorial and chemical events of the Na^+ pump. Panel A shows the empty binding site region with enzyme-bound carboxybiotin (B-COO^-), exposing the Na^+ binding sites toward the cytoplasm. Panel B shows the situation, where the first Na^+ binding site at the D203−N373 pair has been occupied and the second Na^+ enters the S382 site with simultaneous release of the proton from the hydroxyl side chain. The guanidino group of R389 accepts this proton and simultaneously delivers a different proton to the carboxybiotin. This catalyzes the immediate decarboxylation of this acid-labile compound, involving a conformational change (B → C), which exposes the Na^+ binding sites toward the periplasm. The Na^+ ions are subsequently released into this reservoir, while a proton enters the channel and restores the hydroxyl group of S382. In panel D, the Na^+ binding sites are empty and exposed toward the periplasm and the biotin prosthetic group is not modified (B-H). Upon carboxylation of biotin, the protein switches back into the conformation where the Na^+ binding sites are exposed toward the cytoplasm (D → A).

cytoplasm, and conformation 2, in which these sites are open to the periplasm. The catalytic cycle starts by the binding of carboxybiotin, which stabilizes conformation 1. This binding may be supported by charge pairing of the biotin carboxylate with R389, and the biotin carboxylate would therefore penetrate from the cytoplasmic surface into its binding pocket that might be created by the unusual folding of region IIIa (Figure 1B, step D to A; *9*). Further progress of the reaction requires the binding of two Na^+ ions from the cytoplasm to the appropriate amino acid residues on helix VIII and on region IIIa. The first Na^+ ion penetrates the membrane almost completely and binds to D203 (region IIIa) close to the periplasmic surface. The conserved N373 of helix VIII near the periplasmic surface could be an additional ligand of this site. This would be in accord with an almost complete inactivation of oxaloacetate decarboxylase activity in the N373L mutant (Table 1). The complete inactivation of oxaloacetate decarboxylase by the G377A mutation may indicate that G377 of helix VIII is at a critical narrow position of the Na^+-conducting channel or at a critical site of contact with another helix. Possibly, binding of the first Na^+ ion elicits some interhelical rearrangements, by which the binding of the second Na^+ ion to the S382 including site becomes feasible. We propose that upon Na^+ binding to this site, the proton from S382 is abstracted, and enters the proton conduction network including the R389−carboxybiotin pair. The proton of S382 may be transferred to carboxybiotin either directly or via R389 in a simultaneous mechanism as formulated in Figure 6. Cycling of R389 between protonated and deprotonated species (consecutive mechanism) seems less likely, given the high p*K* (12.5) of the guanidino group side chain, but proton release from R389 to carboxybiotin with simultaneous reprotonation of the guanidino group from S382 may be feasible. Upon protonation, the acid-labile carboxybiotin undergoes immediate decarboxylation (step B). The reaction is accompanied by the change to conformation

2 that closes the channel to the cytoplasmic surface and opens it toward the periplasm (step B to C). Once open, the two Na^+ ions bound to the D203- and S382-including sites could then be released through this channel into the periplastic compartment. To displace the Na^+ from S382, a periplasmic proton penetrating through the channel must restore the hydroxyl group of S382 because an uncompensated negative charge would not be tolerated near the center of the membrane for electrostatic reasons. For the proton to reach this deeply embedded membrane position, it could first bind to D203 near the periplasmic surface, thereby releasing the first Na^+ ion, and could be subsequently transmitted to S382 with the release of a second Na^+ ion. An obligatory requirement of D203 and S382 in the proton translocation pathway is compatible with the observation that the decarboxylase activity is completely abolished if either of these residues is mutated (step C). After these events, carboxybiotin formed by OadA by carboxyl transfer with oxaloacetate binds to OadB (step D to A). This stabilizes conformation 1, and a new reaction cycle begins.

Observations in Accord with the Model. In the following, we will give a critical evaluation of experimental data collected over the years with respect to the proposed model.

(i) In the absence of $\Delta\tilde{\mu}Na^+$, the oxaloacetate decarboxylase Na^+ pump operates at a Na^+ to oxaloacetate stoichiometry of about two and one H^+ moves in the opposite direction (*10*, *14*). This observation is in accord with the sequence of events as formulated in Figure 6 (complete reaction cycle from step A to D).

(ii) With a high $\Delta\tilde{\mu}Na^+$, the Na^+ to oxaloacetate stoichiometry drops and the pump catalyzes an exchange of internal and external Na^+ ions (*14*). This observation can be explained if Na^+ is not completely dissociated from the D203−N373 pair to the periplasmic reservoir, due to the high Na^+ concentration at this side. If the conformation changes from 2 to 1 (step D to A) with Na^+ still bound to this site, the Na^+ to oxaloacetate stoichiometry will be reduced. In conformation 1 or 2, the Na^+ at this site may equilibrate with Na^+ ions present in the cytoplasmic or periplasmic compartment, respectively, resulting in the observed exchange of internal and external Na^+ ions.

(iii) Oxaloacetate decarboxylation is inhibited by high Na^+ concentrations, especially at high pH values (*10*). With respect to our model, it is reasonable to assume that these conditions are unfavorable for the H^+-dependent displacement of Na^+ from S382 to the periplasmic surface (step C). Reduction of the reaction velocity by these conditions is therefore expected.

(iv) The pump can be reversed, catalyzing pyruvate carboxylation in the presence of large $\Delta\tilde{\mu}Na^+$ (*29*). The high periplasmic Na^+ concentration triggers Na^+ binding to S382 with exchange for H^+, for which D203 may be required as a base. After binding of the second Na^+, also favored by these conditions, the conformation changes from 2 to 1 and the prosthetic biotin group becomes carboxylated. During this reaction, the proton moves from biotin to S382, thereby releasing the bound Na^+ into the cytoplasm. After dissociation of the second Na^+ into the cytoplasmic reservoir, the carboxybiotin switches from OadB to OadA, where transfer of the carboxyl group to pyruvate yields oxaloacetate (reverse reaction cycle from step D via C and B to A).

(v) The decarboxylation is strictly dependent on Na^+ ions (*30*). In the model, the proton that is consumed in the decarboxylation of carboxybiotin stems from S382, from which it is only released in an exchange with Na^+ and after the second Na^+ binding site on the D203−N373 pair has been occupied with the alkali ion (step C). Accordingly, mutants S382A, -C, -E, -N or -Q, D203E or -N, and N373L that affect the Na^+ coordination geometry are inactive or nearly inactive.

In summary, we present here a molecular model for the coupling of the chemical reaction and the vectorial ion movements across the membrane by the oxaloacetate decarboxylase Na^+ pump. The central feature for this mechanism is using membrane-buried amino acid residues (S382; the D203−N373 pair) as binding sites for the oppositely oriented movements of Na^+ and H^+. The two sites take up Na^+ ions from the cytoplasm and deliver them to the periplasm. Simultaneously, a proton is translocated across the membrane, following the opposite route toward carboxybiotin, where it is consumed in catalyzing the decarboxylation of this acid-labile compound. This model very elegantly describes a direct coupling mechanism, where the Na^+ movement triggers the oppositely oriented translocation of protons across the membrane which directly participate in the chemical event of catalysis.

ACKNOWLEDGMENT

We thank Prof. Etana Padan (Jerusalem, Israel) for sending us *E. coli* EP432. We are grateful to Prof. Lutz Nover (Department of Molecular Cell Biology, Goethe-University, Frankfurt a. M., Germany) for providing the program ImageMaster 1D Prime.

SUPPORTING INFORMATION AVAILABLE

Table A listing the primers used for mutagenesis of the β-subunit. This material is available free of charge via the Internet at http://pubs.acs.org.

REFERENCES

1. Dimroth, P. (1997) *Biochim. Biophys. Acta 1318*, 11−51.
2. Dimroth, P., and Schink, B. (1998) *Arch. Microbiol. 170*, 69−77.
3. Braune, A., Bendrat, K., Rospert, S., and Buckel, W. (1999) *Mol. Microbiol. 31*, 463−472.
4. Hilpert, W., Schink, B., and Dimroth, P. (1984) *EMBO J. 3*, 1665−1670.
5. Dimroth, P., and Hilbi, H. (1997) *Mol. Microbiol. 25*, 3−10.
6. Woehlke, G., Laussermair, E., Schwarz, E., Oesterhelt, D., Reinke, H., Beyreuther, K., and Dimroth, P. (1992) *J. Biol. Chem. 267*, 22804−22805.
7. Laussermair, E., Schwarz, E., Oesterhelt, D., Reinke, H., Beyreuther, K., and Dimroth, P. (1989) *J. Biol. Chem. 264*, 14710−14715.
8. Schwarz, E., Oesterhelt, D., Reinke, H., Beyreuther, K., and Dimroth, P. (1988) *J. Biol. Chem. 263*, 9640−9645.
9. Jockel, P., Di Berardino, M., and Dimroth, P. (1999) *Biochemistry 38*, 13461−13472.
10. Di Berardino, M., and Dimroth, P. (1996) *EMBO J. 15*, 1842−1849.
11. Di Berardino, M., and Dimroth, P. (1995) *Eur. J. Biochem. 231*, 790−801.
12. Dimroth, P., and Thomer, A. (1988) *Eur. J. Biochem. 175*, 175−180.
13. Dimroth, P., and Thomer, A. (1992) *FEBS Lett. 300*, 67−70.

14. Dimroth, P., and Thomer, A. (1993) *Biochemistry 32*, 1734−1739.
15. Yannish-Perron, C., Vieira, J., and Messing, J. (1995) *Gene 33*, 103−119.
16. Pinner, E., Kolter, Y., Padan, E., and Schuldiner, S. (1993) *J. Biol. Chem. 268*, 1729−1734.
17. Dunn, J. J., and Studier, F. W. (1983) *J. Mol. Biol. 219*, 45−59.
18. Sambrook, J., Fritsch, E. F., and Maniatis, T. (1989) *Molecular cloning: A laboratory manual*, 2nd ed., Cold Spring Harbor Laboratory Press, Cold Spring Harbor, NY.
19. Sanger, F., Nicklen, S., and Coulson, A. R. (1977) *Proc. Natl. Acad. Sci. U.S.A. 74*, 5463−5467.
20. Dimroth, P. (1986) *Methods Enzymol. 125*, 530−540.
21. Bradford, M. M. (1979) *Anal. Biochem. 72*, 248−251.
22. Smith, P. K., Krohn, R. I., Hermanson, G. T., Mallia, A. K., Gartner, F. H., Provenzano, M. D., Fujimoto, E. K., Goeke, N. M., Olson, B. J., and Klenk, D. C. (1985) *Anal. Biochem. 150*, 76−85.
23. Krebs, W., Steuber, J., Gemperli, A. C., and Dimroth, P. (1999) *Mol. Microbiol. 33*, 590−598.
24. Nilsson, I. M., and von Heijne, G. (1998) *J. Mol. Biol. 284*, 1185−1189.
25. Dimroth, P. (1982) *Eur. J. Biochem. 121*, 443−449.
26. Dimroth, P., and Thomer, A. (1983) *Eur. J. Biochem. 137*, 107−112.
27. Harel-Bronstein, M., Dibrov, P., Olami, Y., Pinner, E., Schuldiner, S., and Padan, E. (1995) *J. Biol. Chem. 270*, 3816−3822.
28. Paetzel, M., and Dalbey, R. E. (1997) *Trends Biochem. Sci. 22*, 28−31.
29. Dimroth, P., and Hilpert, W. (1984) *Biochemistry 23*, 5360−5366.
30. Dimroth, P., and Thomer, A. (1986) *Eur. J. Biochem. 156*, 157−162.

BI992261V